Modeling of Mutual Coupling between Inductors

G. Asmanis
Institute of Industrial Electronics
Riga Technical University
Riga, Latvia
asmanisgundars@inbox.lv

D.Stepins
Institute of Radio Electronics
Riga Technical University
Riga, Latvia
stepin2@inbox.lv

L.Ribickis, A. Asmanis
Institute of Industrial Electronics
Riga Technical University
Riga, Latvia
leonids.ribickis@rtu.lv, ashmanis@inbox.lv

***Abstract*— This paper is devoted to EMI filter inductor modeling and mutual coupling modeling between two inductors positioned on PCB. 3D inductor models are developed and modeled in CST MWS. Comparison of inductors mutual coupling measurement and modeling results show that transfer coefficients can be predicted accurately. CST MWS has been used also to predict effective mutual coupling reduction techniques.**

***Keywords*— mutual inductance; inductors; modelling; EMI filters; CST MWS.**

I. Introduction

Nowadays all modern electronic devices are equipped with electromagnetic interference (EMI) filters for conducted emission reduction. In order to reduce the size of EMI filters, components such as inductors, are often placed very close to each other. This leads to noticeable mutual couplings which can degrade EMI filter performance [1]. Various measurement techniques for mutual coupling measurements have been proposed in [2], [3]. Extraction of mutual couplings has been discussed in [4], but in [5] – [8] mutual coupling reduction and optimization have been presented. Still, there is insufficient information in the literature [1], [8] about the techniques and possibilities, using in market available, the most popular 3D electromagnetic modeling tools, that could help in more effective manner to solve problems related to inductor-inductor mutual couplings. Despite the fact that there are some articles that have described 3D electromagnetic modeling tools in EMI filter modeling [9] - [11], these are not the industry driven 3D electromagnetic modeling tools. This paper presents modeling of EMI filter inductors and mutual couplings between them using 3D electromagnetic software CST MWS.

II. Prototype PCB for Measurements and Modeling

Two prototype PCB's have been created, for inductance and mutual inductance measurements. The first PCB board is created to measure PCB mounted inductor parameters. One SMA connector is added to enable S-parameter measurements that afterwards can be converted to Z-parameters. PCB prototype and it's 3D model is shown in Fig.1. Second PCB is developed to measure mutual coupling between two inductors. Two SMA connectors are used to measure S-parameters. PCB prototype and 3D model is shown in Fig.2. Models of both prototypes are created in CST MWS [12]. PCB board insulation material is FR4 (loss free). All conductive parts of both models are modeled as perfect electrical conductors (PEC). The insulator for SMA type connector is Teflon (PTFE) (loss free). All 3D model materials are chosen from default material library without any parametric modifications. Second PCB is used to extract mutual inductance between two inductors, mounted on it. Therefore, second PCB 3D model is verified. It is modeled without components, creating high impedance termination for both SMA ports. If inductors are mounted on PCB, they create high impedance termination for both SMA ports, rather than low impedance termination. This is the main reason why open circuit modeling and measurements are done instead of short-circuited modeling and measurements for verification purposes. Results are presented in Fig.3 as forward transfer coefficient S_{21}. Measurement results and modeling results agree very well in whole frequency range.

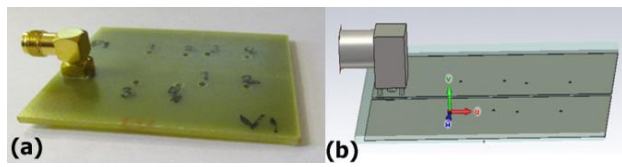

Fig.1. a) PCB prototype for inductor measurements, b) PCB 3D model for modeling in CST MWS.

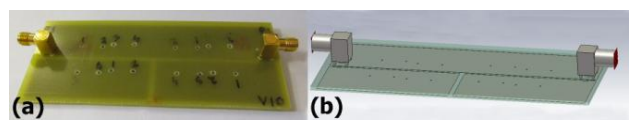

Fig.2 a) PCB prototype for mutual inductance measurements between inductors, b) PCB 3D model in CST MWS.

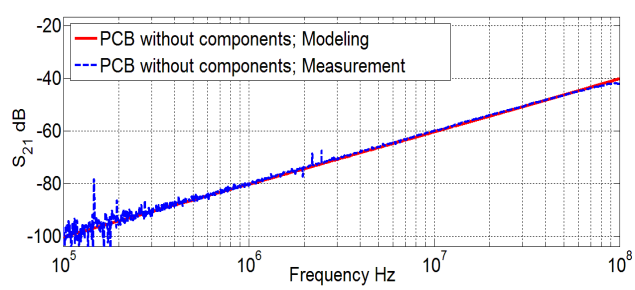

Fig.3 Measurement and modeling results of second PCB without components.

This is a post-print of a paper published in Proceedings of the 2015 IEEE Symposium on Electromagnetic Compatibility & Signal Integrity (EMC&SI 2015) [http://dx.doi.org/10.1109/EMCSI.2015.7107702] and is subject to IEEE copyright.

III. Inductor Modeling and Verification

Conventional inductor is made from couple of windings on core. Core is made from magnetic material or nonmagnetic material. Characterization of inductor with toroid core is complex and time consuming task. Inductor parasitic parameters depends on physical dimensions of inductor components- core material, core size, core insulation thickness, winding wire diameter, winding wire material and insulation thickness, winding turn spacing and winding turn count. Inductor inductance L depends on core material characteristic, winding turns count and distance between core and winding. Parasitic capacitance- EPC, depends on distance between windings and distance between core and windings, including coating material properties of core and winding.

For measurements, inductor core is chosen from Wurth

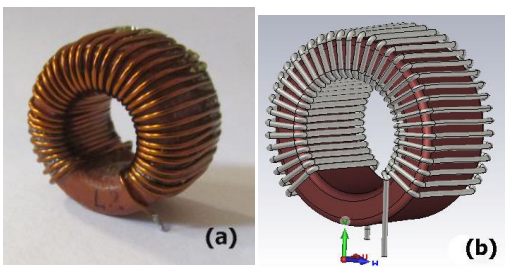

Fig.4 Inductor: a) Measurement prototype, b) CST MSW 3D model.

Elektronik. Wurth Elektronik has provided precise magnetic material characteristics - conductivity and complex magnetic permeability. Core is effectively usable up to 10MHz. The inductor (shown in Fig.4(a)) contains 36 turns winded on toroid core with inner diameter 12mm outer diameter 26mm and core height 16mm. For 3D electromagnetic modeling, inductor model is created Fig. 4(b). In 3D model winding insulation and ferrite core insulation is not modeled, as it will increase mesh cell count drastically, due to the reason that insulation is very thin layer in comparison to other dimensions of inductor. Information provided by Wurth Elektronik can be implemented in toroid core material model, using CST MWS material

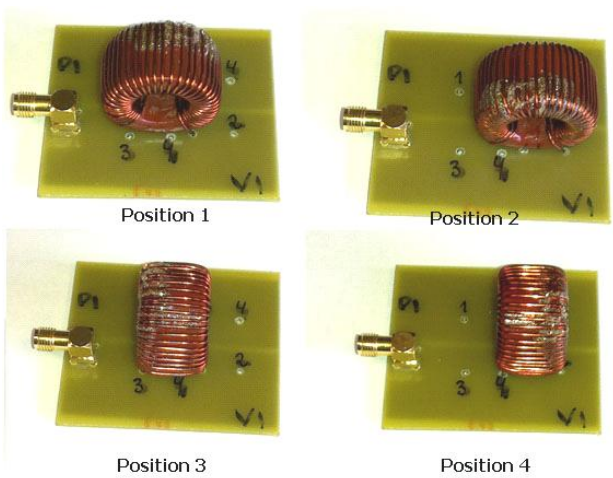

Fig.5 Positions of inductors during measurements.

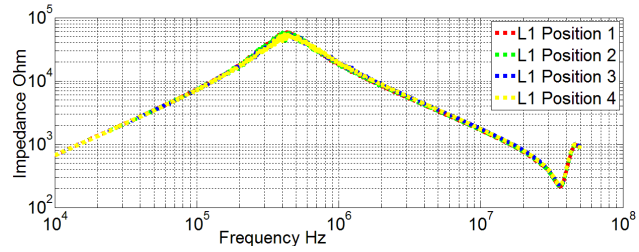

Fig.6 Inductor L1 impedance measurements in four positions.

dispersion property function. As ferrite material is dispersive material (permeability is frequency dependent) it is possible to use only frequency domain solver. Time domain solver does not support dispersive materials. To decrease complexity of inductor model, winding material is defined as PEC - perfect electrical conductor, as we are not interested in DC characteristic and copper losses. Copper substitution with PEC will give negligible effect on modeling results.

To verify PCB and inductor interaction, inductor is placed on PCB in two different positions and rotated by 90 degrees. All four positions are shown in Fig.5. Two identical inductors are measured. Impedance measurements are carried out for both inductors in all four positions. Fig.6 depicts inductor L1 impedance measurement results. Impedance is not changing its characteristic when inductor is moved from position 1 to position 4. Therefore it can be concluded that PCB and inductor interaction gives negligible impact on inductor impedance. The same situation can be observed with inductor L2 - position of inductor has negligible impact on impedance. It should be pointed out that, both inductors- L1 and L2 are made from identical materials and physical dimensions are the same, but impedance of both inductors is not exactly the same. It can be explained by the fact that both inductors are not manufactured identically and have tiny differences, such as- winding turn to winding turn distance, winding turn to core distance.

Modeling results (Fig.7) in CST MSW also give similar results- position of inductor has negligible impact on impedance. In low frequency range 10kHz-100kHz CST MWS do not give results with high accuracy as the model is optimized to deliver precise results in high frequency range. It is possible to optimize the model to deliver more precise results in lower frequency range (up to 100kHz), but in this case the higher frequency range precision will suffer or modeling time will increase. In Fig.8 modeling results are compared with measurement results for inductor position 1. Modeling results fits the measurement results quite well, except the first resonance depth and second resonance frequency. At first

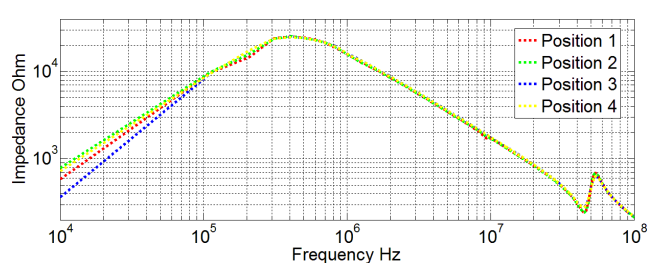

Fig.7 Inductor impedance modeling results in CST MWS.

resonance frequency CST MWS predicts impedance much lower than measurements. The measurements claim 60kOhm while modeling gives 25kOhm impedance at 410kHz frequency. This error is connected to modeling mesh density in the volume between toroid core and winding turns. If mesh density is increased, it is possible to achieve better result fitting, but it dramatically increases the modeling time. The second resonance (at 30-50MHz) is also connected with the mesh density between toroid core and winding turns and 3D model slight inaccuracies.

IV. Mutual Coupling Modeling Between Inductors

For measurements, PCB prototype board, shown in Fig.2 is used. Two inductors (Fig.4) are mounted in three different positions and in two different distances, from each other. All three positions are shown in Fig.9, where inductors are positioned in 30mm distance, from each other (distance is measured from toroid core center). There is also modeled and measured situation, if the inductors are positioned in 55mm distance, from each other. Prototype PCB is connected to two port vector network analyzer and S-parameters are measured. Coupling between the two inductors results in change of S_{21} - forward transfer coefficient. Measurement results compared to modeling results are presented in Fig.10. Measurement results show that there is small difference in S_{21} (few dB), between two distances - 30mm and 55mm. Measurement and modeling results agree very well, even the resonances are modeled quite well in frequency range 20MHz-60MHz. To evaluate which inductor position delivers the worst coupling, measurement

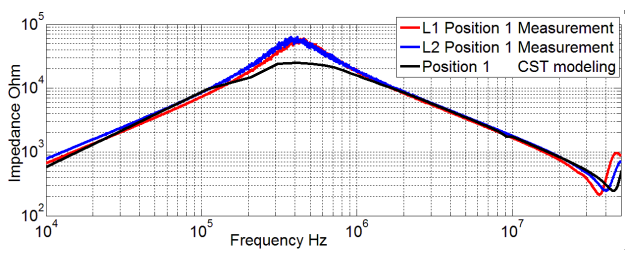

Fig.8. Inductor impedance modeling using inductor 3D model and measurement result comparison.

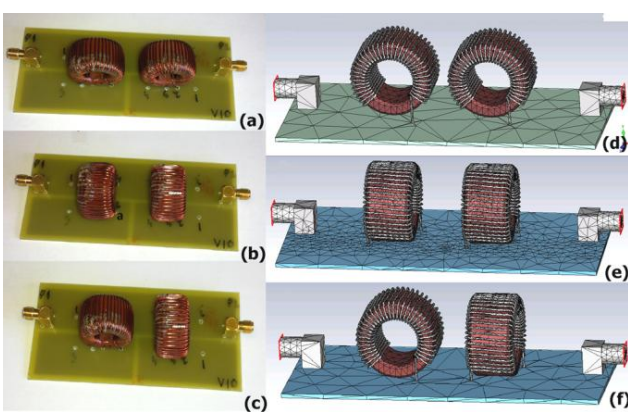

Fig.9. Three different positions of inductors, if distance between them is 30mm: a) Position 1, prototype, b) position 2, prototype, c) position 3, prototype, d) position 1, 3D model, e) position 2, 3D model, f) position 3, 3D model.

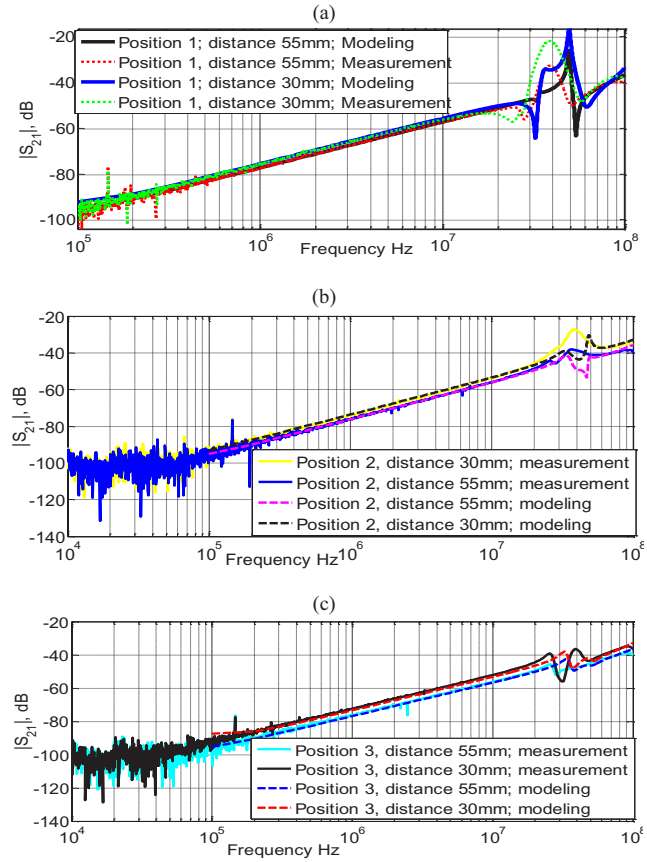

Fig.10. Coupling measurement results and modeling result comparison between two inductors placed in position 1 (a); position 2 (b) and position 3 (c).

results are regrouped in Fig.11. PCB measurement results without inductors mounted on it are included in Fig.11 as a reference. It appears that there is little difference between transfer coefficients S_{21} of all three positions. Position 3 has the highest coupling, but it is only 3dB higher than position 1 transfer coefficient, that appears the worst coupling result. PCB without components provides only 3dB lower coupling than position 1.

These results are not in contrary to recommendations in literature [13] and other, that defines components aligned perpendicularly creates lower coupling. In case of used inductors, component leads are spaced in the way that rotation of component does not considerably change the cross section area in plane between two inductors. Interaction between

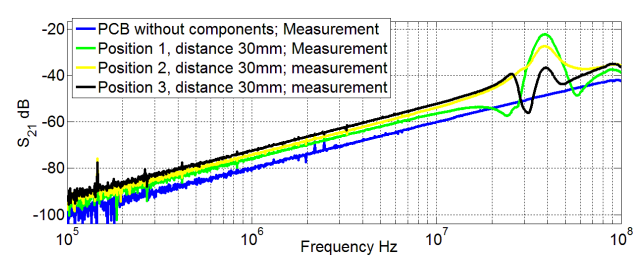

Fig.11. Coupling measurement results between two inductors placed in position1, position 2, position 3 in 30mm distance.

inductors is mainly due to mutual coupling created by inductor leads formed loops, not from inductor itself, as toroidal core is used to keep leakage inductance low. Inductors could be replaced by PEC loops, adding lumped elements in series to represent high inductor impedance. But this approach is not stright forward as in frequency range over couple MHz inductor structure starts to play important role, creating parasitic capacitance to nearby objects. It should be noted that reason of measurements and modeling was not to discover optimized positioning of inductors on PCB, but to verify CST studio usability in mutual coupling modeling between two inductors on PCB. Mutual coupling between two inductors can be analyzed in sense of impedance. The coupling complex impedance can be calculated in frequency domain exploring measured circuit as two port T-type network and applying equation as follows [2]

$$Z_{mc} = \frac{2Z_0 \cdot S_{21}}{(1 - S_{22} + S_{22}S_{11} - S_{11} - S_{21}^2)}. \qquad (1)$$

Impedance is calculated for Position 1, when inductors are positioned in 30mm. Impedance results are compared in Fig.12. Calculated impedance acquired by measuring and modeling results fits quite well in whole frequency range, except near ~30MHz, where impedance resonance is not modeled very accurately. It appears that impedance is not purely inductive. To verify impedance characteristic, impedance phase angle is calculated for both- measured and modeled results and represented in Fig.13. Measured and calculated impedance phase angle results agree quite well, except at 30MHz range where impedance resonances appear and in kHz range where abrupt phase switching occurs. Measurement results are noisy at the very beginning of measurements. Phase angle higher than $|90^0|$ could be explained by the fact that circuit acts as transformer in frequency range up to 50kHz. Up to 1MHz impedance performs inductively. In frequency range 1MHz-20MHz impedance has capacitive character. Afterwards couple of

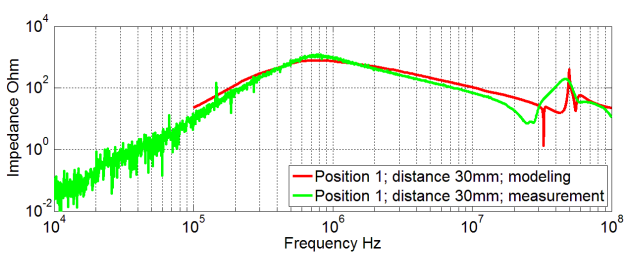

Fig.12. Mutual coupling impedance Z_{mc} magnitude in Position 1; 30mm distance.

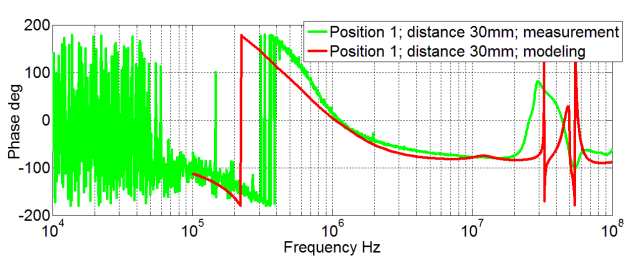

Fig.13. Mutual coupling impedance angle in Position 1; 30mm distance.

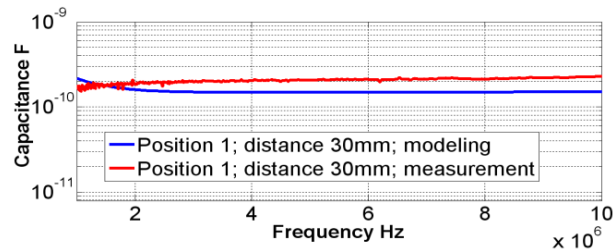

Fig.14. From measurement and modeling results extracted parasitic capacitance C_{mc}; Position 1; 30mm distance.

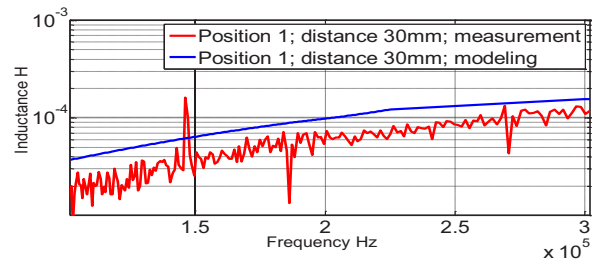

Fig.15. From measurement and modeling results extracted parasitic mutual inductance L_{mc} between two inductors; Position 1; 30mm distance.

resonances occurs with abrupt phase changes. Therefore, it can be concluded that coupling between two inductors has mutual inductance and parasitic capacitance in parallel. Parasitic capacitance can be explained by the fact that PCB has its self-parasitic capacitance. If inductors are placed on PCB, extra stray capacitance is added. As X_c is dominating in frequency range 1MHz-10MHz, it can be calculated as follows

$$C_{mc} = \frac{1}{2\pi f \,|\, Z_{mc}(f) \,|}, \qquad (2)$$

C_{mc} measurement and modeling results are presented in Fig.14. It appears that calculated capacitance C_{mc} is well predicted by the modeling results. In the same manner inductive impedance component can be calculated in impedance range where X_L is dominating, using the following expression

$$L_{mc} = |\, Z_{mc}(f_1) \,| \,/\, 2\pi f_1, \qquad (3)$$

where f_1 is frequency in linear region of $|Z_{mc}(f)|$. Calculated mutual inductance L_{mc} is presented in Fig.15. Calculated mutual inductance results from measured and modeled S-parameter results agree very well.

Inductive component can also be calculated using Thompson equation, but it can be also used to verify accuracy of calculated inductive and capacitive components, in case of parallel resonance, calculating resonance frequency. Calculation results are verified using Thompson equation. Resonance frequency is predicted ~1MHz. Therefore, it can be concluded that mutual coupling can be well predicted and analyzed, using CST MSW. In position 1, when inductors are positioned in 30mm distance, extracted mutual inductance is 0.1uH and parasitic capacitance 227pF at 2MHz frequency. Inductance value is slightly changing in frequency range.

In Fig.16 and Fig.17 mutual inductance and capacitance is presented for all three inductor positions. If two inductors are

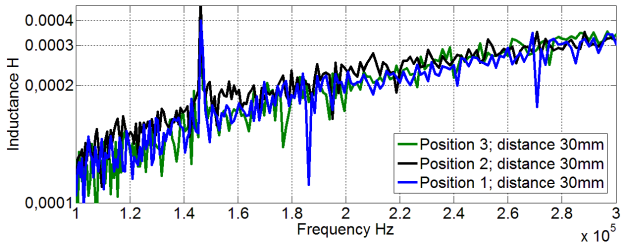

Fig.16. From measurement results extracted mutual inductance between two inductors positioned in 30mm distance.

placed in 30mm distance Position 1 shows the lowest coupling, while Position 2 provides the highest mutual inductance, however difference between extracted results is small. If two inductors are placed in 50mm distance Position 2 shows the lowest coupling, while Position 3 provides the highest mutual inductance. In contrary to 30mm inductor distance, difference between mutual couplings is reasonable. Also parasitic capacitance results are inductor position and placement distance dependent, Fig.17. The highest parasitic capacitance is provided by Position 1, when inductors are positioned in 50mm distance. The lowest parasitic capacitance is provided by Position 3 when inductors are placed in 50mm distance. Upper stated measurement results do not give clear answer for the question: "Which position gives the lowest coupling".

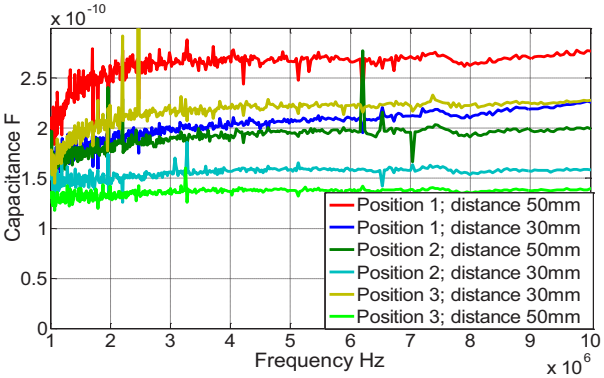

Fig.17. From measurement results extracted parasitic capacitance.

V. Mutual Coupling Reduction Between Two Inductors

It is possible to reduce mutual coupling between two inductors mounted on PCB in close distance, using various techniques. One of the possibilities is to use shielding between two inductors and ground plane on PCB. There are analyzed three mutual inductance reduction techniques:

1) application of ground plane (GND);
2) application of ground plane and shielding (shielding is raised 1mm above ground plane and connected in two points to the ground plane);
3) application of ground plane and shielding (shielding is soldered to the ground plane in whole length).

All three shielding technique 3D models are presented in Fig.18 to Fig.20. 3D models are represented as surface current modeling results, to give overview of shielding technique

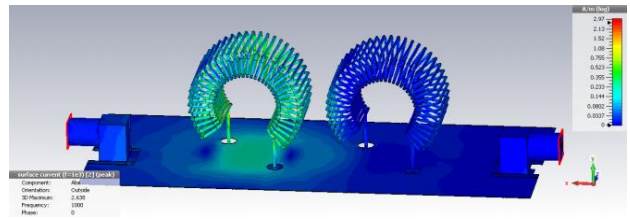

Fig.18. Surface current modeling in CST MSW- mutual coupling reduction using ground plane.

impact on surface currents and close fields. Inductor ferrite cores are not shown in 3D models as surface current is modeled only in conductors. Initiating left inductor on PCB, it is clearly visible, that surface current is present on the ground plane below inductor and in nearby (right) inductor windings, if the shielding is not installed, Fig.18. If shielding is installed and connected in two points to ground plane, surface current is not induced in nearby (right) inductor windings, but surface current is penetrating through slot created by shielding and ground plane – Fig.19. If shielding is soldered to the ground

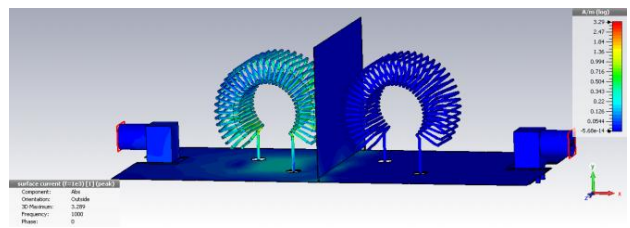

Fig.19. Surface current modeling in CST MSW- mutual coupling reduction using ground plane and shielding connected in two points.

plane in whole length surface current is present only on the excited inductor side (left inductors on PCB) – Fig.20.

Transmission coefficient S_{21} modeling results, clearly supports surface current modeling results. S_{21} modeling results are presented in Fig.21. Ground plane usage, has a little role in mutual coupling cancelation, if shielding is not applied. Shielding between two inductors reduces coupling by at least 10dB and connection style (connection in two points or in whole length) has negligible effect on transfer coefficient. Modeling results predicts measurement results very well in whole frequency rage, with static 6dB offset (modeled transfer coefficient is 6dB higher than measurement results). Up to 1MHz measured transfer coefficient results are noisy, due to the vector network analyzer noise floor. Mutual coupling between two inductors can be analyzed in sense of impedance. The coupling impedance can be calculated in frequency

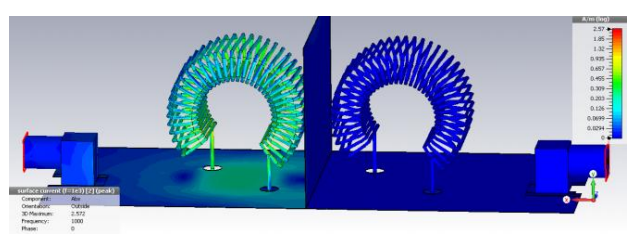

Fig.20. Surface current modeling in CST MSW- mutual coupling reduction using ground plane and shielding soldered in whole length.

domain using (1). In case if only ground plane is used measurement and modeling results in Fig.22 agree quite well in inductive impedance region- up to 300kHz. In capacitive impedance region- 800kHz to 200MHz, modeling results predicts higher impedance than measured one. This can be explained by the fact that modeling predicts lower parasitic capacitance component. Both impedance resonances are predicted with high accuracy. In case if shielding is used in addition to ground plane for mutual coupling reduction, impedance in inductive region is predicted slightly lower than measurement results, due to the fact that predicted mutual inductance is slightly lower than measured mutual inductance.

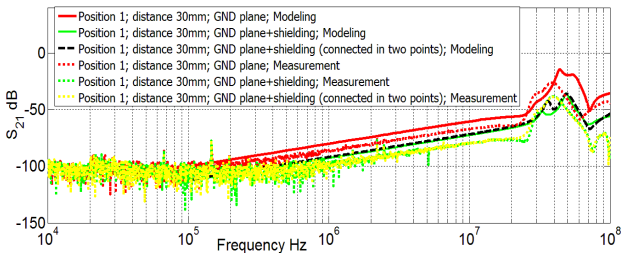

Fig.21. Transfer coefficient $|S_{21}|$, modeling and measurement result comparison for different mutual coupling cancelation techniques.

In capacitive impedance region impedance using modeling is not predicted with high accuracy. Predicted parasitic

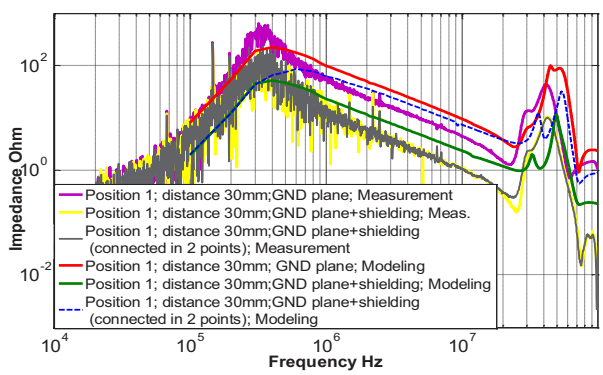

Fig.22. Mutual coupling impedance magnitude, extracted from measurement and modeling results.

capacitance is lower than measured. Impedance resonance frequencies are predicted quite well.

Modeling results in case of ground plane and shielding has higher error, than in case without these solid structures. Carrying out multiple repeated measurements there was discovered that transfer coefficient S21, is sensitive to small variations of component positioning in respect to PCB ground plane and shielding. Prediction of measurement results could be improved, if 3D model of whole structure were more precise, representing models with all tiny sags. For further EMI filter modeling, 3D model precision should be considered as critical to closely predict measurement results.

VI. Conclusions

There exist coupling between two inductors positioned on PCB. Interaction between inductors is mainly due to mutual coupling created by inductor leads formed loops, not from inductor itself, as toroidal core is used to keep leakage inductance low. Inductors could be replaced by PEC loops, adding lumped elements in series to represent high inductor impedance. But this approach is not stright forward as in frequency range over couple MHz inductor structure starts to play important role, creating parasitic capacitance to nearby objects. Inductor positioning has negligible impact on coupling magnitude, but this conclusion cannot be extended to other situations as coupling strongly depends on inductor impedance. In cases, if inductor has low inductance, positioning can have considerable impact on coupling. Comparison of inductors mutual coupling measurement and simulation results show that transfer coefficients can be predicted with high accuracy using CST MSW modeling. It is possible to use CST to predict mutual coupling reduction techniques. Prediction error is strongly dependent on 3D model precision if in close proximity solid large conductive structures are positioned, such as PCB ground plane and shielding, as well as EMI filter enclosure. It is possible to successively use CST MSW in EMI power filter inductor impedance, mutual coupling and mutual coupling reduction technique analysis.

References

[1] G. Asmanis, A. Asmanis, and D. Stepins, "Mutual couplings in three phase T-type EMI filters," in 2012 International Symposium on Electromagnetic Compatibility (EMC EUROPE), Rome, 2012, pp. 1-6.

[2] S. Wang, Lee, F.C., Odendaal W.G., "Characterization and Parasitic Extraction of EMI Filters Using Scattering Parameters," IEEE Transactions on Power Electronics, March 2005, pp. 502 – 510.

[3] G. Asmanis, A. Asmanis, and L. Ribickis, "Analysis of high frequency effects in three phase EMI filters," in 2012 Asia-Pacific Symp. on Electromag. Compatibility (APEMC), Singapore, 2012, pp. 653-656.

[4] F. C. Lee, D. Y. Chen, W. G. Odendaal, and Shuo Wang, "Effects of Parasitic Parameters on the Performance of EMI Filters," IEEE Trans. on Power Electronics, vol. 19, no. 3, pp. 869-877, May 2004.

[5] T. Oliveira, J. Schanen, J. Guichon, and L. Gerbaud, "Automatic layout optimization of an EMC filter," in 2010 IEEE Energy Conversion Congress and Exposition (ECCE), Atlanta, GA, 2010, pp. 2679-2685.

[6] T. Oliveira, J. Schanen, J. Guichon, J. Roudet, and L. Gerbaud, "PEEC-Models for EMC filter layout optimization," in 2010 6th Int. Conf. on Integrated Power Electronics Systems (CIPS), Nuremberg, 2010, p. 6.

[7] T. Oliveira, J. Schanen, J. Guichon, and J. Roudet, "Optimized layout for an EMC filter: Analysis and validations," in 2012 Int. Symp. on Electromagnetic Compatibility (EMC EUROPE), Rome, 2012, p. 6.

[8] S. Wang, R.Chen, and F. C. Lee, "Improved passive filter configurations for high-frequency conducted EMI in power electronics," in 2005 Europ. Conf. on Pow. Electron. and Applications, Dresden, 2004, p. 16.

[9] I. F. Kovacevic, T. Friedli, A. Musing, and J. W. Kolar, "PEEC-based virtual design of EMI input filters," in 2011 IEEE Energy Conversion Congress and Exposition (ECCE),, Phoenix, AZ, 2011, pp. 1935-1941.

[10] I. F. Kovacevic, T. Friedli, A. M. Musing, J. W. Kolar, "3-D Electromagnetic Modeling of Parasitics and Mutual Coupling in EMI Filters," IEEE Tran. Pow. Elect., vol. 29, no. 1, pp. 135-149, Jan. 2014.

[11] I. F. Kovacevic, T. Friedli, A. M. Muesing, and J. W. Kolar, "Electromagnetic Modeling of EMI Input Filters," in 2012 7th International Conference on Integrated Power Electronics Systems (CIPS), Nuremberg, 2012, p. 9.

[12] CST microwave studio workflow & solver overview.: CST, 2013.

[13] Shuo Wang, F.C. Lee, W.G. Odendaal, and J.D. van Wyk, "Improvement of EMI Filter Performance with Parasitic Coupling Cancellation," in Power Electronics Specialists Conference, Recife, 2005, pp. 1780 - 1786.